J. Membrane Biol. 187, 85–96 (2002)
DOI: 10.1007/s00232-001-0154-6

The Journal of
Membrane
Biology

Modulation of Renal Type IIa Na^+/P_i Cotransporter Kinetics by the Arginine Modifier Phenylglyoxal

I.C. Forster, K. Köhler, G. Stange, J. Biber, H. Murer
Physiologisches Institut, Universität Zürich-Irchel, Winterthurerstr. 190, CH-8057, Switzerland

Received: 3 October 2001/Revised: 28 January 2002

Abstract. The effects of the arginine-modifying reagent phenylglyoxal on the kinetics of the type IIa Na^+/P_i cotransporter expressed in *Xenopus*, oocytes were studied by means of $^{32}P_i$ uptake and electrophysiology. Phenylglyoxal incubation induced up to 60% loss of cotransport function but only marginally altered the Na^+-leak. Substrate activation and pH dependency remained essentially unaltered, whereas the voltage dependency of P_i-induced change in electrogenic response was significantly reduced. Presteady-state charge movements were suppressed and the equilibrium charge distribution was shifted slightly towards hyperpolarizing potentials. Charge movements in the absence of external Na^+ were also suppressed, which indicated that the empty-carrier kinetics were modified. These effects were incorporated into an ordered alternating access model for NaPi-IIa, whereby the arginine modification by phenylglyoxal was modeled as altered apparent electrical distances moved by mobile charges, together with a slower rate of translocation of the electroneutral, fully loaded carrier.

Key words: Arginine modification — Cotransport — *Xenopus* oocyte — Electrophysiology

Introduction

The type IIa renal Na^+/P_i cotransporter (NaPi-IIa) is an electrogenic, Na^+-driven cotransporter responsible for mediating transluminal P_i transport in the mammalian proximal tubule (Murer et al., 2000). Its macroscopic electrogenic properties can be explained by two putative mechanisms consistent with an alternating access model: (i) intrinsic charges associated with the NaPi-IIa protein, the movement of which leads to the occlusion or exposure of co-substrate (Na^+) binding sites and (ii) movement of Na^+ ions to their binding site within the transmembrane electric field (Forster et al., 1998; Forster, Biber & Murer, 2000).

Currently, the residues and/or regions of the NaPi-IIa protein involved in mediating these mechanisms have not been identified. One approach to the identification of functionally important sites in membrane transporters involves chemical modification of amino-acid residues within the protein. Neutral cysteine and charged (e.g., arginine, lysine and histidine) residues can be targeted by specific externally applied reagents or modified by the local ionic environment. If accessible, and functionally important, the modified residue(s) are expected to confer quantifiable changes to the transport properties. For example, we have applied the substituted cysteine accessibility method (SCAM) (Karlin and Akabas, 1998) to the renal type IIa Na^+/P_i cotransporter expressed in *Xenopus* oocytes to identify a putative P_i transport pathway (Lambert et al., 1999b, 2001; Köhler et al., 2001).

By analogy with the proposed mechanisms involved in ion channel gating (e.g., Bezanilla, 2000), charged amino acids, located within the transmembrane electric field, are also likely to be involved in conferring voltage dependence to electrogenic cotransporters. To test this hypothesis, we investigated the effects of the arginine-modifying reagent phenylglyoxal (PG) on the wild-type (WT) NaPi-IIa transport kinetics. This study was legitimated by previous investigations that documented a significantly reduced $^{32}P_i$ uptake of renal brush border membrane vesicles after exposure to PG (Strévey, Brunettes & Beliveau, 1984; Strévey et al., 1992). Since the type IIa cotransporter is now established as the key element in renal Na^+-dependent P_i transport (Beck et al., 1998;

Correspondence to: I.C. Forster; email: iforster@access.unizh.ch

Murer et al., 2000), it is anticipated that the most likely target protein in both these studies on native membranes would have been NaPi-IIa. Moreover, our recent finding that a mutant NaPi-IIa construct (R462C) showed significantly altered voltage dependence (Lambert et al., 2001) indicates that at least one arginine residue is involved in determining the electrogenic properties of the NaPi-IIa protein.

By expressing NaPi-IIa in *Xenopus* oocytes, we confirmed that PG treatment also led to a loss of cotransport activity comparable with that reported for the native membrane preparation. Substrate activation, pH dependency and Na^+-leak current of NaPi-IIa were essentially unaffected by PG treatment, whereas the voltage dependency of steady-state P_i-induced current and of the presteady-state relaxations was altered. These effects could be described analytically as changes of two parameters of an 8-state ordered model for NaPi-IIa: (i) altered apparent electrical distances moved by mobile charges and (ii) decelerated rates of the electroneutral translocation of the fully loaded carrier. Interestingly, two mutant transporters (R210C, R462C) still showed decreased transport rates after PG treatment, which implied that these arginine residues alone are not the functionally relevant targets for PG.

Materials and Methods

Reagents and Solutions

All standard reagents were obtained from either Sigma or Fluka (Buchs, Switzerland). The solution compositions (in mM) were as follows:

(i) oocyte incubation (modified Barth's solution): NaCl, 88; KCl, 1; $CaCl_2$, 0.41; $MgSO_4$, 0.82; $NaHCO_3$, 2.5; $Ca(NO_3)_2$, 2; HEPES, 7.5; adjusted to pH 7.6 with TRIS and supplemented with antibiotics (10 mg/l gentomycin, streptomycin).
(ii) control superfusate (ND100): NaCl, 100; KCl, 2; $CaCl_2$, 1.8; $MgCl_2$, 1; HEPES, 5, and adjusted to pH 7.4 with KOH.
(iii) control superfusate with X mM Na^+ substitution (NDX): As for ND100, but with N-methyl-D-glucamine to replace (100-×) % of Na^+. Solution adjusted to pH 7.4 with HCl.
(iv) phenylglyoxal (PG) incubation solution was prepared from a PG stock (3 M) in DMSO and diluted to the final concentration in ND100 with pH adjusted to 8.5–9.0 with KOH (***see*** Strévey et al., 1992).
(*v*) substrate test solutions: inorganic phosphate (P_i) was added to control superfusate from 1 M K_2HPO_4 and KH_2PO_4 stocks that were mixed to give the required pH. Phosphonoformic acid (PFA) was added from frozen stock (100 mM) to give 3 mM final concentration and the pH was adjusted to 7.4.

Oocyte Handling

The procedures for oocyte preparation and cRNA injection have been described in detail (Werner et al., 1990). Oocytes were injected with either 50 nl of water or 50 nl of water containing 10 ng of cRNA. Oocytes were incubated in modified Barth's solution and the experiments were performed 3–4 d after injection. For most experiments, pooled data were obtained from oocytes from at least two different donor frogs. For the standard 20-min incubation in PG, oocytes were either transferred from the recording chamber to a multiwell dish for the incubation period or were maintained in the recording chamber with PG applied via a 0.5-mm dia. cannula. In the latter case, washout of incubation medium for at least 1 min was performed before retesting the cell response. We confirmed that this was adequate by exposing an oocyte to PG for a shorter time period (10 min). After washout, the response to repeated application of P_i did not change, which indicated that the reaction did not proceed further for the given exposure conditions (*data not shown*).

Functional Assays

Radiolabeled P_i Uptake

This procedure has been described in detail elsewhere (Werner et al., 1990). $^{32}P_i$ uptake was measured 3 d after injection in water-injected (control) and cRNA-injected oocytes ($n = 5$).

Electrophysiology and Data Analysis

The standard two-electrode voltage-clamp technique was used as previously described (Forster et al., 1998). Unless otherwise indicated, the steady-state response of an oocyte to P_i was always measured at a holding potential (V_h) = −50 mV in ND100 solution. Data were acquired on-line using pClamp v. 8.0 and Digidata 1200A hardware (Axon Instruments, Foster City, CA), with sampling conditions compatible with the signal bandwidth. Data were analyzed using routines supplied with Clampfit v. 8 (Axon Instruments) and/or Prism v. 3.2 software (Graphpad Software, SanDiego, CA). Current-voltage (*I–V*) curves were obtained by applying a series of voltage steps of 60 ms duration to the test potential from $V_h = -60$ mV. The P_i-dependent currents were obtained by subtracting corresponding records obtained in ND100 from those obtained in ND100 + P_i (1 mM). Na^+-dependent leak current was obtained by subtracting corresponding records in ND100 + PFA (3 mM) from ND100 records. This same voltage-step protocol was used to obtain presteady-state relaxations, except that the low-pass filter setting was increased (typically 0.5 kHz). Presteady-state relaxations were fit with a single decaying exponential using a Chebychev transform-based algorithm (Axon Instruments). Charge movements were described by a Boltzmann relation:

$$Q = Q_{hyp} + Q_{max}/(1 + \exp(-ze(V - V_{0.5}/kT)) \quad (1)$$

where Q_{max} is the maximum charge translocated, Q_{hyp}, is the steady-state charge at the hyperpolarizing limit and depends on V_h, $V_{0.5}$ is the voltage at which the charge is distributed equally between the depolarizing and hyperpolarizing limits, z is the apparent valency per cotransporter, e, k, and T have their usual thermodynamic meaning. Eqn. 1 was fit to the data by nonlinear regression analysis. To take account of different expression levels, *Q–V* data were pooled according to the following procedure: the *Q–V* data for each cell were offset by the predicted Q_{hyp}, and then normalized to Q_{max} in ND100. For some batches of oocytes a linear baseline correction was applied to eliminate contamination from Ca^{2+}-activated Cl^- currrents for voltage steps to $V \geq +40$ mV. All data are shown as mean ± SEM.

Results

Phenylglyoxal Incubation Promotes Loss of NaPi -IIa Cotransport Capacity

Oocytes expressing NaPi-IIa and incubated in phenylglyoxal (PG) (30 mM, pH 8.5) for 20 min,

typically showed a 50% loss in $^{32}P_i$ uptake compared with the control group (Fig. 1*A*). These were similar to the PG-incubation conditions employed by Strévey et al. (1984) and Strévey et al. (1992) using renal brush border membrane vesicles (BBMVs). This result confirmed their basic findings and indicated that the type IIa Na^+/P_i cotransporter, present in BBMVs, was the most likely target for PG action in these native renal membranes. We also documented a loss of electrogenic activity of individual oocytes under voltage-clamp conditions: typically, a 60% decrease in P_i-induced current (1 mM P_i, $V_h = -50$ mV) was recorded under the same PG-incubation conditions (Fig. 1*B*) used for the uptake assay. Moreover, the loss of function was stable for at least 30 min after incubation (*data not shown*), which suggested that PG had induced a permanent alteration in the NaPi-IIa protein kinetics.[1]

Since $^{32}P_i$ uptake and electrogenic activity are tightly correlated (Forster et al., 1999a), these findings indicated that we could use the electrogenic activity as a valid read-out for possible functional modulation by PG. Therefore, in all subsequent experiments, functional assays were made exclusively by electrophysiology.

The loss of transport function documented in Fig. 1 may have resulted from a retrieval of transporters from the membrane induced by the PG treatment. If this were the case, we would expect a decrease in the oocyte membrane area because induced membrane-protein retrieval is commonly accompanied by endocytotic events that involve incorporation or removal of plasma membrane (e.g., Wright et al., 1997). We therefore measured the oocyte membrane capacitance (an indirect measure of membrane area (e.g., Hirsch, Loo & Wright, 1996; Forster et al., 1999b) using a voltage-step protocol as we previously reported (Forster et al., 1999b). No significant alteration in membrane capacitance was observed (*data not shown*). Therefore, we concluded that the PG action was a result of altered NaPi-IIa transport kinetics.

Strévey et al. (1984) reported a time- and concentration-dependence of the PG effect on $^{32}P_i$ uptake in BBMVs. As the efficacy of PG action might differ depending on the membrane properties of the expression system and the specificity of the proteins mediating P_i transport in the case of BBMVs, we therefore determined the optimal incubation conditions for NaPi-IIa expressed in *Xenopus* oocytes. A dose-dependency assay was performed for individual oocytes with the P_i-induced current (I_{P_i}) recorded at 5-min intervals at three concentrations of PG (Fig. 1*C*). With incubation in 30 mM PG, activity decreased asymptotically to approximately 40% of the initial value. Superimposed on these data are the corresponding data points taken from Fig. 1 in Strévey

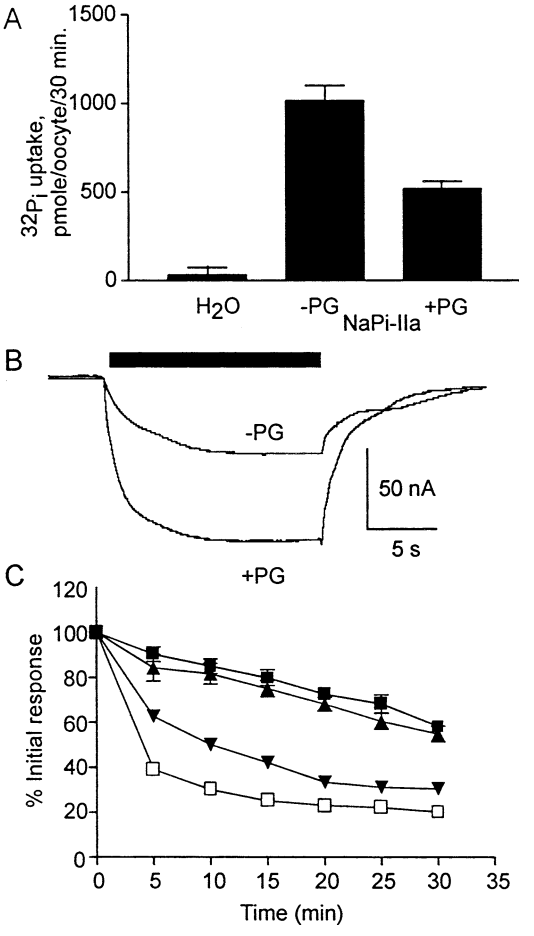

Fig. 1. PG incubation suppresses P_i transport by NaPi-IIa expressed in *Xenopus* oocytes. (*A*) Effect on $^{32}P_i$ uptake of incubating oocytes in 30 mM phenylglyoxal (PG). Uptake was measured under standard conditions (1 mM P_i, 100 mM Na^+, pH 7.4). Water-injected oocytes were from the same batch. (*B*) Suppressed $^{32}P_i$ transport is also reflected in the P_i-induced electrogenic response (100 mM Na^+, $V_h = -50$ mV), for the same representative oocyte before (−PG) and after (+PG) incubation. P_i, (1 mM) was applied during the period indicated by the bar. (*C*) Time dependency of the PG effect at three concentrations of PG. The P_i-induced electrogenic response was measured at 5-min intervals and normalized to the control response at the start: 5 mM PG (*filled squares*); 10 mM PG (*filled triangles*); 30 mM PG (*filled inverted triangles*). Data from Fig. 1 (Strévey et al., 1984, reproduced with permission from authors, Biochem J. 223: 793–802. 1984.) for 30 mM PG incubation of renal brush border membrane vesicles have been superimposed (*open squares*). Each point is the mean ± SEM ($n = 3$). Standard errors smaller than symbol are not shown.

[1]Exposure of NaPi-IIa-expressing oocytes to the vehicle under the standard incubation conditions (1% DMSO, pH 8.5; osmolarity increased by 30 mOsmol, without PG) for the same time period did not result in a significant loss of electrogenic activity, other than that which could be accounted for by normal rundown (typically <15% of initial response) with repeated exposure to P_i (Forster et al., 1999b) (*data not shown*). Moreover, exposure of non-injected oocytes to the same incubation conditions (with or without PG) did not induce significant response to substrates (P_i or PFA), which may otherwise have led to a contamination of the results for NaPi-IIa expressing cells (*data not shown*).

et al. (1984), also using 30 mM PG. The time course was similar, but for the oocyte preparation, the plateau was approximately 10% higher than for the BBMV assay. In all subsequent experiments we incubated oocytes for typically 20 min in 30 mM PG as a standard procedure (*see* Materials and Methods).[1]

Effect of PG Incubation on NaPi-IIa Steady-State Transport Kinetics

We next investigated whether the loss of function could be accounted for by PG altering one or more of the NaPi-IIa kinetic fingerprints such as pH, substrate activation and voltage dependence. A change in any one of these properties could alone, or in combination, lead to a deviation from the WT behavior, which might provide clues as to the mechanism of PG action.

Proton and Substrate Interaction

Figure 2*A* shows representative recordings from the same oocyte, which illustrate the effect of PG incubation on the pH dependency of NaPi-IIa. As previously documented, decreasing external pH leads to a significant loss of electrogenic activity under standard test conditions (100 mM Na^+, 1 mM total P_i, V_h = −50 mV), which reflects a direct interaction of protons with the NaPi-IIa protein and competition for Na^+ binding, in addition to the altered availability of the preferred species of P_i (HPO_4^{2-}) (Forster et al., 1999a; 2000). After PG incubation, the same behavior was also observed, which suggested that under these conditions, the interaction of protons with NaPi-IIa was unchanged. This is quantitated in Fig. 2*B* as the response at pH 6.2 relative to pH 7.4. Similarly, substrate activation was not significantly altered after PG treatment: with 100 mM external Na^+, the change in response to a 10-fold reduction in P_i from near saturation (1 mM) to 0.1 mM—a value close to the established apparent P_i affinity ($K_m^{P_i} = 0.06$ mM, Forster et al., 1998)—remained unchanged (Fig. 2*B*). Furthermore, the response to 1 mM P_i at two Na^+ concentrations (25 mM and 50 mM), relative to that at 100 mM Na^+ was also only marginally affected after PG treatment (Fig. 2*B*). Taken together, these findings suggested that PG did not appear to alter the interaction of either substrate or protons with the NaPi-IIa protein.

Steady-State Voltage Dependence of P_i Activation

To obtain the P_i- dependent current (I_{P_i}) we adopted the usual procedure to eliminate endogenous currents (Forster et al., 1998) by subtracting the response in ND100 from that in ND100 + P_i (1 mM). Fig. 3*A* shows a typical set of difference-current records before and after PG treatment for a representative oocyte in response to voltage steps to test potentials in the range −120 to +20 mV from V_h = −60 mV. For steps to potentials outside this range, some oocytes showed contamination from Ca^{2+}-activated Cl^- currents that made estimation of the steady-state current less reliable. The relaxations to the new steady-state current plateau represent presteady-state charge movements and reflect the rearrangement of mobile charges within the transmembrane electric field in response to changes in the externally applied membrane potential (*see* below). When the steady-state current was reached, the plateau current after PG treatment was significantly reduced at all test

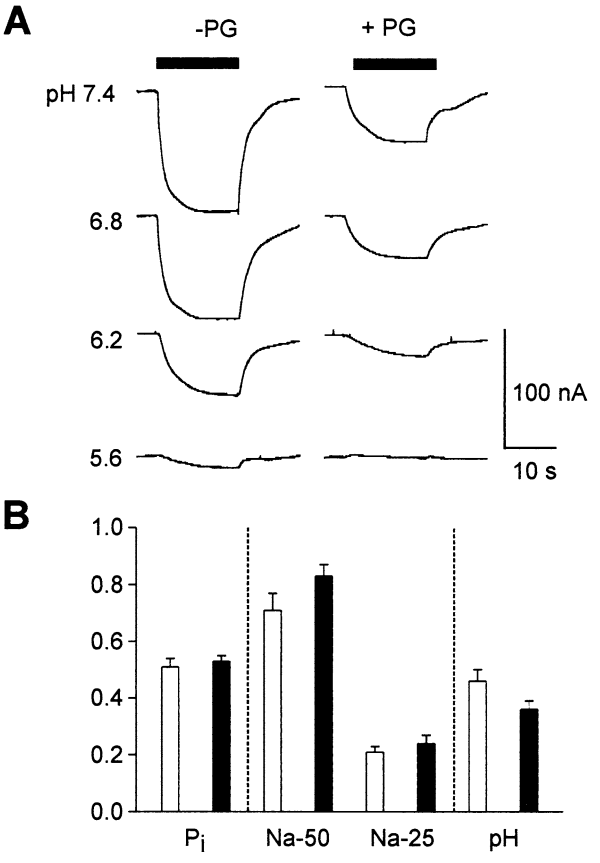

Fig. 2. Interaction of protons and substrate with NaPi-IIa remains intact after PG incubation at V_h = −50 mV. (*A*) Representative recordings from the same oocyte before (−PG) and after (+PG) incubation under standard conditions (*see* text). P_i-induced currents were recorded in presence of ND100 solution adjusted to pH values indicated. P_i (1 mM total) was applied during the period indicated by the bars. The baseline current was recorded at the indicated pH in each case. (*B*) Summary of the relative effects of changing substrate and external protons on NaPi-IIa steady-state kinetics: −PG (*open bars*); +PG (*filled bars*). Legend labels: P_i: ratio of current induced by 0.1 mM P_i to 1 mM P_i (100 mM Na^+) (n = 4); *Na-25*: ratio of current at 25 mM Na^+ to 100 mM Na^+ (1 mM P_i) (n = 6); *Na-50*: ratio of current at 50 mM Na^+ to 100 mM Na^+) (1 mM P_i) (n = 4); pH: ratio of current at pH 6.2 to pH 7.4 (100 mM Na^+, 1 mM total P_i) (n = 4). Each data point in the pooled set was obtained from one oocyte measured before and after PG exposure under the different substrate test conditions.

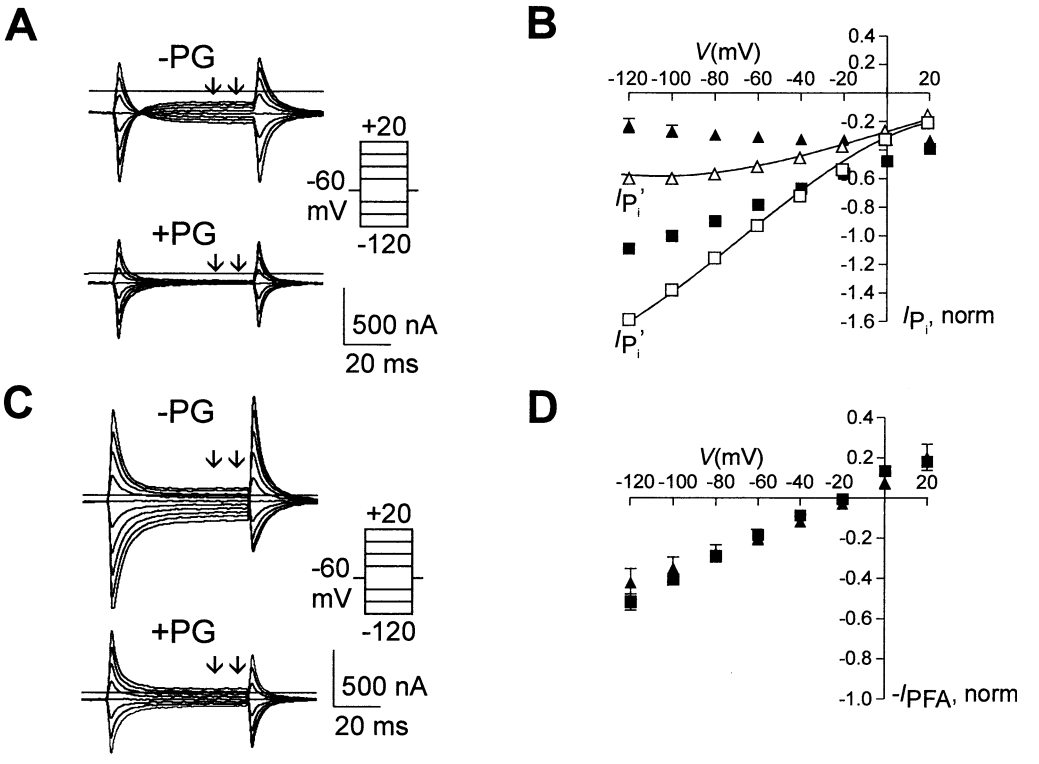

Fig. 3. Steady-state voltage dependency and PG treatment. (*A*) Current records from one representative cell obtained in response to voltage steps applied according to the protocol shown. The mean current between the arrows was taken as the steady-state current at the corresponding test potential, before (−PG) and after (+PG) incubation. Each record was obtained by subtracting the response in ND100 from the corresponding response in ND100 + P_i (1 mM). Records were digitally filtered at 200 Hz (4-pole Bessel characteristic) and each is the average for 4 consecutive sweeps. Continuous line represents zero P_i-induced current level. (*B*) Current-voltage (*I–V*) relation for data pooled from two batches of oocytes (n = 4 per batch). Data from each cell were normalized to the difference current at −100 mV before PG treatment. Open symbols were obtained by correcting the P_i-induced current for Na^+-leak and represent the true cotransport current magnitude (I_{P_i}') (*see* text). (*C*) Voltage-step records obtained from the same oocyte as in *A* for the PFA-dependent current before (−PG) and after (+PG) incubation in PG. Each record was obtained by subtracting the response in ND100 + PFA (3 mM) from the corresponding response in ND100. Same recording conditions as in *A*. (*D*) Current-voltage (*I–V*) relation for the Na^+-dependent leak or PFA-sensitive current ($-I_{PFA}$) for data pooled from the same two batches of oocytes as in *C*. Data from each cell were normalized to the corresponding P_i-dependent current at −100 mV before PG treatment.

potentials. Steady-state current-voltage (*I–V*) curves were obtained before and after PG treatment on the same oocyte and to take account of different expression levels, the data were then pooled by normalizing each data set to the response at −100 mV before PG treatment. Compared with the control response, the normalized *I–V* data after PG treatment showed a dramatically flattened dependency on V over the voltage range -120 mV $< V <$ +20 mV. The maximum (I_{P_i}) was reduced by ~60% of that observed at the hyperpolarizing extreme (−120 mV), before PG treatment. For most batches of oocytes the P_i-activation *I–V* relation showed a negative slope in the hyperpolarizing potential range

Steady-State Voltage Dependence of Na^+-Leak

In the absence of external P_i, NaPi-IIa exhibits a Na^+-leak current (slippage mode) (Forster et al., 1998) that can be detected by using the Na^+/P_i transport blocker phosphonoformic acid (PFA). We quantitated this leak current ($-I_{PFA}$) using PFA as previously described (*see* Materials and Methods) before and after PG treatment, by subtracting the response to PFA (3 mM) from each record in ND100 alone. Current records from the same oocyte as in Fig. 3*A* are shown for this protocol in Fig. 3*C*. Data sets for each oocyte were then normalized to the P_i-induced current at −100 mV and pooled. The two sets of pooled data before and after PG treatment superimposed reasonably well in the voltage range -80 mV $< V <$ +20 mV (Fig. 3*D*). This indicated that, in contrast to I_{P_i}, the Na^+-leak current was only marginally affected by the PG treatment. Moreover, we observed only a small change in the reversal potential (< 10 mV). This finding suggested that the driving-force conditions had not altered after PG treatment. A more precise determination of reversal potential was not possible because of sensitivity of the subtraction procedure to contamination from chan-

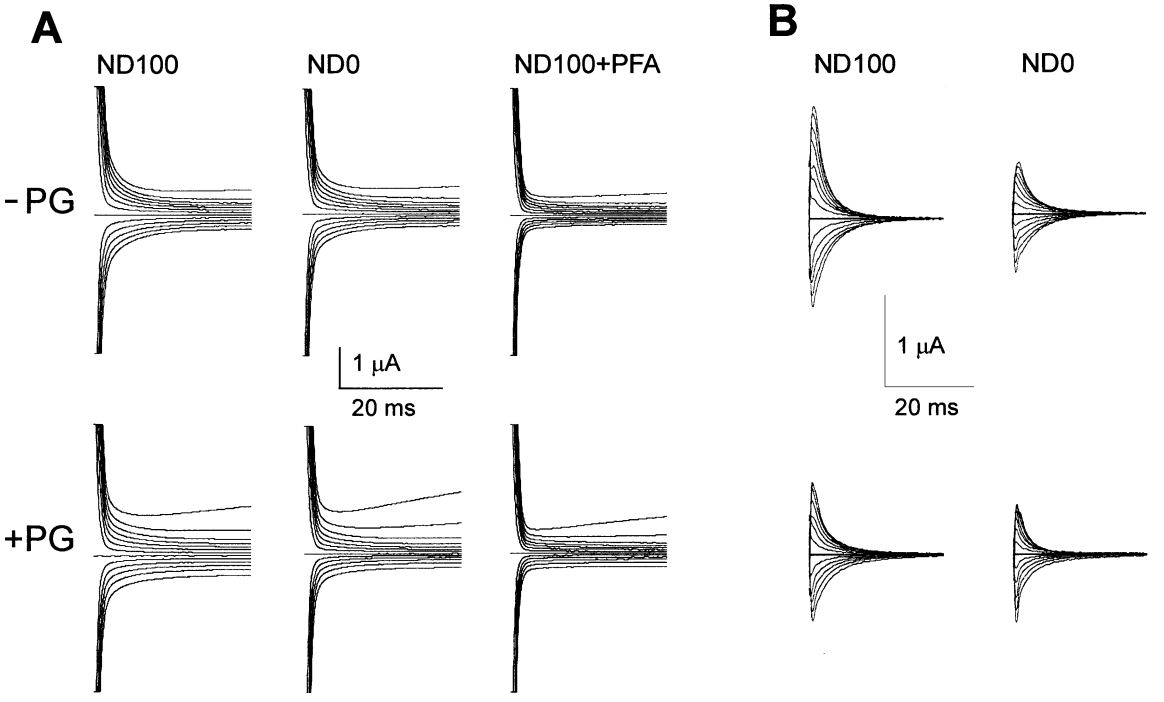

Fig. 4. PG incubation alters presteady-state kinetics of NaPi-IIa in ND100. (*A*) ON-transient currents recorded in response to voltage steps in the range −160 mV to +80 mV before (−PG) and after (+PG) treatment for the same cell. Records in ND100 (*left*); ND0 (*center*) and ND100+PFA (3 mM) (*right*) are shown. The time-dependent outward current component for steps to +60 mV and +80 mV is due to activation of endogenous Ca^{2+}-activated Cl^- currents. Each record is the result of averaging 4 sweeps, filtered at 500 Hz. (*B*) difference records obtained from the raw data in *A* by subtracting the PFA records from the corresponding record in ND100 (*left*) or ND0 (*right*). Note that the vertical scale is different from that in *A*. All steady-state currents were removed with baseline correction.

Table 1. Fit parameters for single Boltzmann fit (Eqn. 1) to presteady-state *Q–V* data for superfusion in ND100 and ND0 ($n = 6$)

Fit parameter	ND100		ND0	
	−PG	+PG	−PG	+PG
$V_{0.5}$ (mV)	−66 ± 2	−117 ± 10	−78 ± 3	−123 ± 10
z	−0.47 ± 0.02	−0.46 ± 0.03	−0.48 ± 0.03	−0.49 ± 0.03

ges in the endogenous response between successive current measurements. The deviations at higher and lower voltages most likely reflect contamination from time-dependent endogenous Ca^{2+}-activated Cl^- currents that were not fully suppressed by the subtraction procedure.

Correcting I_{P_i} for Leak Current

The current kinetic model for NaPi-IIa (*see* Fig. 7*A* and Forster et al., 1998) assumes that the Na^+-leak is uncoupled from the cotransport mode. This means that at saturating P_i, the Na^+-leak current does not contribute to the measured cotransport-mode current. According to the standard procedure used to obtain I_{P_i} described above, the P_i-induced current is measured relative to the baseline current in ND100. This current comprises two components: the endogenous currents and the NaPi-IIa Na^+-leak. The subtraction method used to obtain I_{P_i} eliminates the latter (Fig. 3*A,B*) but will underestimate the true P_i-induced cotransport current by an amount equal to the Na^+-leak. The corrected P_i-induced currents, given by: $I_{P_i'} = I_{P_i} - I_{PFA}$ (Fig. 3*B, continuous lines, open symbols*), indicate that after PG treatment voltage dependency was restored to $I_{P_i'}$: within the voltage range $-80 < V < 0$ mV, the slope was positive as for the −PG case, but nevertheless reduced. Moreover, at hyperpolarizing potentials, the flattening of the corrected *I–V* curve for the +PG case suggests that voltage-independent rate-limiting steps dominate the cotransport kinetics and thereby lead to a reduced maximum transport rate.

Effect of Phenylglyoxal on Presteady-State Kinetics

Altered steady-state voltage dependency induced by PG should be reflected in NaPi-IIa presteady-state

charge movements (e.g., Forster et al., 1998, 2000). Indeed, a reduction in charge movement is suggested from the PFA-dependent currents after PG treatment (Fig. 3*C*). Representative records over a wider voltage range (−160 mV to +80 mV) for the ON transitions obtained from the same cell before and after PG treatment are shown in Fig. 4*A*. As these relaxations are proposed to arise from charge movements associated with the movement of free Na^+ ions within the transmembrane electric field, as well as the intrinsic charges associated with the empty carrier, we recorded them in full Na^+ (ND100, *left*) and zero Na^+ (ND0, *center*) to distinguish between a PG effect on Na^+ binding alone and/or the empty carrier. To facilitate analysis and remove contamination from endogenous oocyte currents, we also recorded the cell response to ND100 + PFA (3 mM) (*right*), whereby we assumed that at this concentration, only endogenous transient current would remain (Forster et al., 1998; 2000). We observed no significant change in the transient currents under PFA superfusion conditions following PG treatment, except for the appearance of slow outward currents at the extreme depolarizing potential. These are commonly associated with the activation of endogenous Ca^{2+}-activated Cl^- currents. This effect was dependent on the oocyte batch, but since it was paralleled in all superfusion conditions after PG treatment (Fig. 4*A*), it was significantly suppressed after subtraction of the ND100 + PFA records from the ND100 and ND0 records, respectively (*see* Materials and Methods). Fig. 4*B* shows the result subtracting the ND100 + PFA records from the ND100 and ND0 raw data. For this cell, PG treatment resulted in a clear alteration in the presteady-state kinetics (amount of charge and time course of relaxations) under both superfusion conditions. Moreover, the relaxation rates at hyperpolarizing potentials (< −60 mV) appeared decelerated.

The altered charge movement was quantified by integrating the difference-current records to estimate the total charge moved from V_h to the test potential (Fig. 5*A*). In full Na^+, the most obvious effect of PG was to reduce significantly the maximum charge movement at the depolarizing extreme, whereas the tendency of the *Q–V* data to saturate at hyperpolarizing limit was also absent. This same qualitative trend was also seen for ND0 superfusion. This finding suggested that PG treatment resulted in a hyperpolarizing shift of the voltage dependence of the intrinsic (empty carrier) charge movement. These effects were consistent in batches of oocytes from different donor toads.

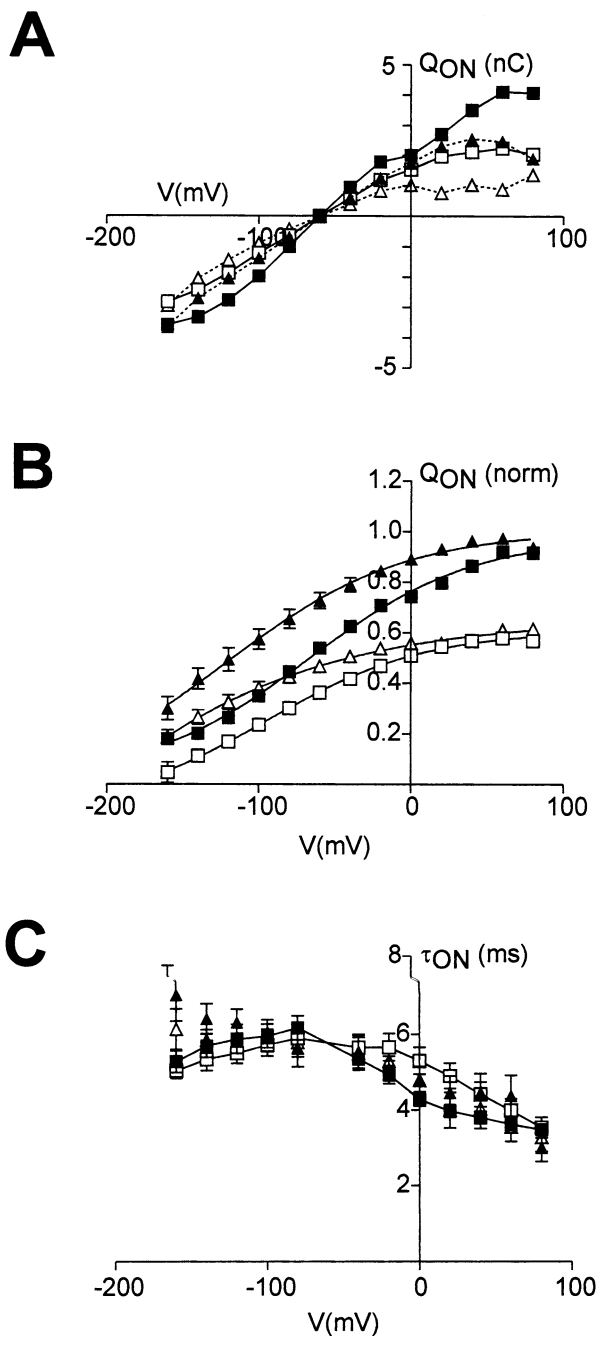

Fig. 5. Analysis of presteady-state currents in ND100 and ND0 (*A*) Integration of difference records to obtain ON charge movement for the same cell as Fig. 4*A* before (*squares*) and after (*triangles*) PG treatment for the case of superfusion in ND100 (*filled symbols*, *continuous lines*) and ND0 (*open symbols; broken lines*). (*B*) Normalized, pooled *Q–V* data ($n = 6$). For each cell, the charge-voltage (*Q–V*) relation was first determined as shown in *A* and the data were manipulated as described in Materials and Methods. Symbols: ND100 (*filled symbols*); ND0 (open *symbols*); −PG (*squares*) and +PG (*triangles*). Continuous curves are fits of Eqn. 1 to the rescaled data. The fit parameters were as follows: ND100, −PG: $V_{0.5} = -66.3$ mV, $z = -0.47$; ND100, +PG: $V_{0.5} = -122$ mV, $z = -0.43$; ND0, −PG: $V_{0.5} = -94.5$ mV, $z = -0.48$; ND0, +PG: −250 mV, $z = -0.29$. (*C*) Voltage dependency of main relaxation rate (τ-*V*), determined by fitting single-exponential data to the ON difference currents as in Fig. 4*B*, commencing approximately 2 msec after application of the voltage step. Each data point is the mean ± SEM ($n = 6$). Same symbols as for *B*. −PG data points have been joined to aid identification.

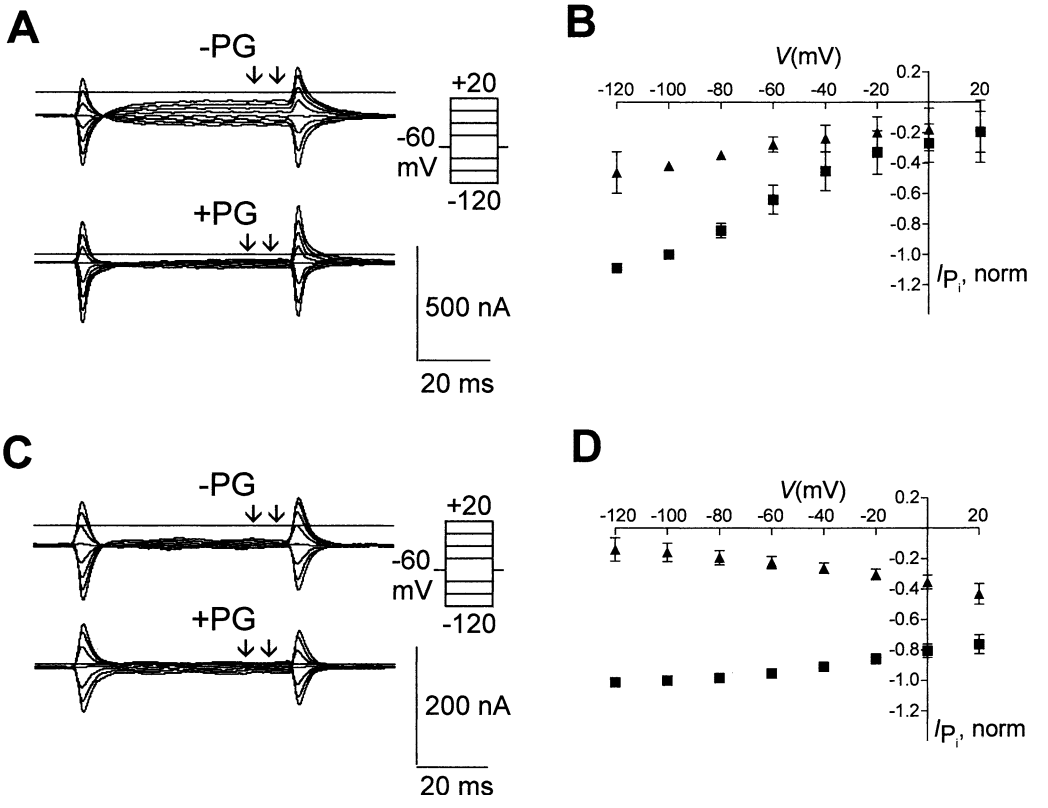

Fig. 6. Effect of PG treatment on steady-state *I–V* relations for two mutant constructs. (*A*) Current records from a representative cell expressing the construct R210C, obtained in response to voltage steps applied according to the protocol shown. The mean current between the arrows was taken as the steady-state current at the corresponding test potential before (−PG) and after (+PG) incubation. Each record was obtained by subtracting the response in ND100 from the corresponding response in ND100 + P_i (1 mM). Records were digitally filtered at 200 Hz (4-pole Bessel characteristic) and each is the average for 4 consecutive sweeps. Continuous line represents zero P_i-induced current level. (*B*) Current-voltage (*I–V*) relation for the R210C. Data from each cell were normalized to the difference current at −100 mV before PG treatment ($n = 3$). (*C*) Current records from a representative cell expressing the construct R462C, obtained in response to voltage steps applied according to the protocol shown. Data processing as for *A*, with filtering for this cell at 20 Hz . (*D*) Current-voltage (*I–V*) relation for R462C. Data from each cell were normalized to the difference current at −100 mV before PG treatment ($n = 3$).

To quantify further these changes in presteady-state kinetics, we applied two curve-fitting procedures. First, the charge movement voltage dependence was quantified by fitting a single Boltzmann function (Eqn. 1) to obtain a measure of the midpoint potential ($V_{0.5}$) and apparent valency (z). Data were pooled from two batches of oocytes (*see* Methods and Materials). The normalized *Q–V* data pooled from 6 oocytes is shown in Fig. 5*B*. The pooled fit parameters for the individual oocytes (Table 1) confirmed that for both ND100 and ND0 superfusion conditions, PG incubation led to a shift of $V_{0.5}$ towards hyperpolarizing potentials, whereas no significant change in z was documented. Moreover, in ND100, the ratio of Q_{max} before and after PG treatment remained close to unity (0.96 ± 0.01, $n = 6$).

Second, we quantified the rate of relaxation in terms of a single exponential decay by curve fitting (Fig. 5*C*). The voltage dependency of the ON-time constant (τ_{ON}) before PG treatment for both superfusion conditions showed the usual "bell"-shaped characteristic that we have previously reported (Forster et al., 1998, 2000). This displays a peak in the range −60 to −80 mV that corresponds well with the midpoint voltage obtained from the *Q–V* fit. After PG treatment, the data points in the depolarizing region showed little deviation from the case without PG for either superfusion condition. In the hyperpolarizing region, no clear maximum for τ_{ON} was observed over the voltage range tested, although the spread in estimates of τ_{ON} was greater in this region. This behavior also supported the altered *Q–V* characteristics and was consistent with the notion that PG treatment had led to hyperpolarizing shift in the equilibrium of the charge distribution.

PG Suppresses P_i-induced Response of Mutant Constructs R210C and R462C

During the course of cysteine-scanning studies of NaPi-IIa (Lambert et al., 2001; Köhler et al., 2002), two functional mutant cotransporters were synthe-

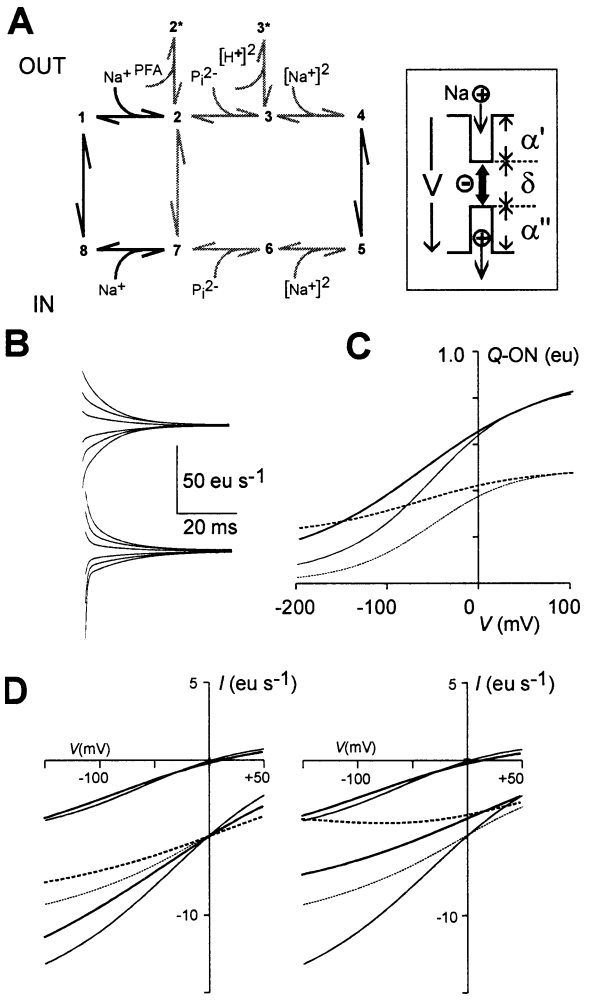

Fig. 7. Modeling and identification of PG-sensitive kinetic transitions in an 8-state alternating-access model for NaPi-IIa. (*A*) An 8-state kinetic model for NaPi-IIa. Kinetic transitions hypothesized as likely transitions modified by PG are shown bold. Boxed inset depicts the lumped charge movements: negatively charged empty carrier and movement of Na^+ ions to and from binding sites within the transmembrane field, corresponding to steps 1↔8, 1↔2 and 7↔8, respectively. For simulations, the parameters used for the control condition were: $k^0_{12} = 2000\ M^{-1}s^{-1}$; $k^0_{21} = 200\ s^{-1}$; $k^0_{23} = 1000\ mM^{-1}s^{-1}$; $k^0_{32} = 1000\ s^{-1}$; $k^0_{34} = 10^6\ M^{-2}s^{-1}$; $k^0_{43} = 1000\ s^{-1}$; $k^0_{45} = 25\ s^{-1}$; $k^0_{54} = 25\ s^{-1}$; $k^0_{27} = 7\ s^{-1}$; $k^0_{18} = 120\ s^{-1}$; $k^0_{81} = 30\ s^{-1}$; $k^0_{56} = 1000\ s^{-1}$; $k^0_{65} = 10^5\ M^{-2}s^{-1}$; $k^0_{67} = 1000\ s^{-1}$; $k^0_{78} = 500\ s^{-1}$; $k^0_{87} = 10^4\ M^{-1}s^{-1}$; where k^0_{ij} is the rate constant at $V = 0$ for the transition from state *i* to *j*. Rates k_{72} and k_{76} were constrained by the microscopic reversibility condition. A single negative charge is translocated by the empty or fully loaded carrier. Equivalent electrical distances moved by charges (*see* inset) are: δ (empty carrier), α'' (external Na^+ binding) and α'' (internal Na^+ binding) so that $\alpha' + \delta + \alpha'' = 1$. Then, $z_{12} = -1$ $\alpha' = -0.25$; $z_{18} = 1$; $\delta = -0.5$, $z_{87} = -1$, $\alpha'' = -0.25$, where z_{ij} is the apparent valency for the transition i↔j (*see* Appendix in Forster et al. (2000) for more details). The temperature was taken as 20°C; external P_i = 3 mM. Internal Na^+ = 20 mM and internal P_i = 1 mM, were chosen to give a reversal potential close to 0 mV for PFA-sensitive current. (*B*) Presteady-state relaxations predicted using model for voltage jumps from $V_h = -60$ mV in 40-mV intervals from −180 mV, for control condition (*upper*) and when apparent valencies are changed to: $z_{12} = -0.35$, $z_{18} = -0.3$ and $z_{78} = -0.35$ (*lower*). (*C*) Voltage dependency of presteady-state charge distribution (Q–V) for parameters corresponding to those used to generate relaxations in *B:* control (*thin curves*); altered apparent valencies (*thick curves*). Total charge (*continuous curves*); charge distribution for transition 1↔8 (*broken curves*). (*D*) Simulated steady-state I–V curves. *Left*: effect of changing only apparent valencies $z_{12} = -0.35$, $z_{18} = -0.3$ and $z_{78} = -0.35$ (*bold traces*). *Right:* effect of an additional reduction in rates of fully loaded carrier transition k_{45}, k_{54} from 25 s^{-1} to 12.5 s^{-1}. Dashed traces in each case are P_i-dependent current with Na^+ -leak subtracted, as would normally be recorded by subtracting the response in ND100 from that in ND100 + P_i. In each case, control conditions (equivalent to −PG) using parameter set in *A* are shown by *thin* traces. Note that for all simulations, the charge movements were evaluated for a single NaPi-IIa molecule, in electron units (*eu*), where 1 *eu* = 1.602×10^{-19}C.

sized in which cysteine residues were substituted for the native arginine at sites 210 and 462, respectively. We reasoned that if either of these native arginines were responsible for the PG effects, the electrogenic kinetics of these constructs (R210C, R462C) would remain unchanged after PG exposure. Fig. 6*A* shows a representative set of P_i-dependent currents before (−PG) and after (+PG) treatment in response to voltage steps in the range −120 mV to +20 mV for the mutant R210C. This mutant showed a WT-like voltage dependency for I_{P_i} which was suppressed by approximately 50% after PG treatment, as shown in the I–V curves normalized to $V_h = -100$ mV, as previously described for the WT (Fig. 6*B*). Application of the same protocol to a representative oocyte expressing the R462C (Fig. 6*B*) showed significantly reduced voltage dependency for I_{P_i} as previously reported (Lambert et al., 2001). As the pooled I–V data confirm (Fig. 6*D*), after PG treatment, the P_i-induced current was further suppressed. These findings allowed us to exclude Arg-210 and Arg-462 as primary targets for PG action.

Discussion

The effect of arginine modification by PG on membrane protein function has been reported in several preparations including frog myelinated nerve (Meves, Rubli & Stämpfli, 1988), frog skeletal muscle (Etter, 1990) and membrane charge movements in hippocampal pyramidal cells (Chameau, Bournard & Shimahara, 1995), as well as organic (Strévey et al., 1984) and inorganic substrate transport in brush border membrane vesicles (Strévey et al., 1984; Strévey et al., 1992). In all these studies, which include both ion channels and secondary-active cotransporters, the common observation was that PG incubation caused an irreversible loss of function of the transport systems under study. The general conclusion is that PG directly targets arginine residues responsible for conferring the transport/gating properties of the re-

spective proteins. In our investigation we have established that the reported suppression of $^{32}P_i$ uptake after PG treatment of renal BBMV's (Strévey et al., 1984; Strévey et al., 1992) can be best accounted for in terms of a direct action of PG on the type IIa Na^+/P_i cotransport protein. The small discrepancy in maximum inhibition between our data and that for BBMVs might be due to P_i transport via systems other than NaP_i-IIa that are also suppressed by PG. The present study complements these earlier studies by taking advantage of: (i) heterologous expression of NaPi-IIa in *Xenopus* oocytes to minimize contamination from other membrane proteins and (ii) the electrogenic properties of NaPi-IIa kinetics to focus on transitions in the transport cycle that might be PG targets.

Accessory proteins that interact with a membrane-transport protein might also be potential targets for PG action. Through their regulatory action on the target protein (e.g., leading to phosphorylation/dephosphorylation at functionally critical sites), transporter kinetics could be modulated. For example, altered stoichiometry of the Na^+-bicarbonate cotransporter kNBC1 due to serine phosphorylation has been recently described (Gross et al., 2001). For NaPi-IIa, no evidence for modulation of kinetics through phosphorylation exists. Moreover, no associated proteins have so far been identified that might subserve a role of modulating the transport kinetics. In the absence of findings to the contrary, we therefore assume that the reported PG action on NaPi-IIa is a result of modification of one or more native arginine residues in the NaPi-IIa protein itself. In the present study, the nonspecific targeting of membrane proteins other than NaPi-IIa by PG was evidenced by an increase in endogenous Ca^{2+}-activated Cl^- currents after PG treatment. This effect appeared to be strongly dependent on oocyte batch. In the absence of any functional correlation between these endogenous currents and heterologously expressed NaPi-IIa kinetics, we assumed that the two proteins are functionally independent.

NaPi-IIa contains 29 arginines, of which the majority (24) are located in predicted intracellular linker regions between transmembrane domains and the intracellular N-terminal and C-terminal tails, respectively (Lambert et al., 1999b). The remaining 5 arginines are located in the large extracellular loop between the 3rd and 4th transmembrane domains. Interestingly, none of the arginines is located in a predicted transmembrane domain, which, by analogy with ion channel topologies (e.g., the *shaker* potassium channel [Bezanilla, 2000]), one might expect if they were to act as sensors of the membrane potential. Moreover, Strévey et al. (1992) have argued that the PG effect on BBMVs is most likely targeted to an Arg residue located in the cytosol. Recent structure-function studies using SCAM applied to transporter proteins have revealed the importance of predicted linker regions in forming transport pathways and determining electrogenic properties. As a result of such reentrant topology, charged arginines, predicted to lie outside the transmembrane region, may indeed act as sensors of the transmembrane electric field or interact with other charged residues within the transmembrane domains. Reentrancy of linkers with functional implications has been proposed for NaPi-IIa (e.g., Lambert et al., 2001; Köhler et al., 2002), the glutamate transporter (GLT-1) (e.g., Brocke et al., 2002) and the sodium-coupled glucose cotransporter (SGLT-1) (e.g., Silverman, 2000). From our present study, we can reject two candidates (R210, located in the putative 1st intracellular linker and R462, located in the putative 3rd extracellular linker) as sites for PG action based on direct experimental evidence. Further mutagenesis, beyond the scope of the present work, will be required to test the remaining 27 arginines.

Incorporating PG Effects into an Alternating Access Model for NaPi-IIa

The kinetic scheme depicted in Fig. 7*A* accounts for the steady-state and presteady-state kinetics of NaPi-IIa expressed in *Xenopus* oocytes (Forster et al., 1998, 2000). This is an alternating access model with ordered substrate binding derived from the scheme described by Parent et al. (1992) for the SGLT-1. Can we predict which transitions might be candidate targets for PG action, based on our findings? Since the rate of translocation of substrate is in general a function of the rates associated with all kinetic transitions, a large degree of freedom exists for identification of candidate transitions. However, as discussed below, the altered steady-state and presteady-state kinetics after PG treatment allowed us to exclude certain transitions and concomitantly identify likely candidates for PG targeting.

First, simulations using this model indicate that transitions $2\leftrightarrow3$ and $3\leftrightarrow4$, which involve external binding of P_i and two Na^+ ions, respectively, are strong determinants of the apparent affinities for these substrates on the periplasmic side of the membrane. Since substrate activation is little affected by PG, we excluded these transitions as PG targets. Similarly, the pH dependency was intact and therefore the interaction of protons with the final Na^+-binding transition ($3\leftrightarrow3^*$) could be excluded. Moreover, the interaction of PFA appeared unchanged, which implies that step $2\leftrightarrow2^*$ is also unaffected.

Second, the altered presteady-state kinetics after PG treatment suggested focussing on voltage-dependent transitions that contribute to these charge movements. The shift in the mid-point potential ($V_{0.5}$) of the Q–V data could result from changes to the kinetic parameters associated with transitions in

the loop 1↔2↔7↔8↔1. For example, qualitatively similar behavior is observed when the external Na^+ concentration is reduced, which would alter the rate of transition 1↔2 (Forster et al., 1998). However, in the absence of external Na^+, altered kinetics were also observed, which would support the hypothesis that the empty carrier itself was the target for PG (transition 1↔8). Indeed, our simulations showed that a reduction in the apparent electrical distance (δ) moved by the lumped charge associated with the empty carrier (*see* Inset, Fig. 7*A*) could best account for these findings. With a 40% reduction in δ, and corresponding increases in the electrical distances associated with Na^+-binding (i.e., to satisfy the model constraint: $\alpha' + \alpha'' + \delta = 1$), simulations showed that the main relaxation was little changed for depolarizing voltage steps, consistent with the τ–V data (Fig. 7*B*). In the hyperpolarizing direction, a fast component was revealed that was superimposed upon a slower relaxation. This was also suggested from the measurements (Fig. 4*B*), however, given the bandwidth limitations of the measuring system, which were not taken into account in the simulations [2] quantification of this fast component would not be straightforward. Finally, the predicted total Q-V data (Fig. 7*C*) confirmed the measured behavior for both full-Na^+ and zero-Na^+ conditions.

Can these changes to empty carrier kinetics explain the observed steady-state behavior? Since the only transition involving charge translocation is 1↔8, we would expect a reduction in δ to give a decreased maximum slope for the voltage dependency of the steady-state I–V data. Simulations revealed this to be the case (Fig. 7*D*, *left*) and only a marginal alteration in the Na^+-leak component was also predicted. However, we were unable to fully account for the measured decrease in voltage dependence without an extreme reduction in δ, which then resulted in significant changes in both Na^+-leak and total Q–V, inconsistent with observation. Moreover, at 0 mV, we generally observed a reduction in the electrogenic response, not predicted by changes in δ (*see* Fig. 7*C*, *left*), which would indicate modification of zero-voltage rate constants. One likely candidate transition for additional modification by PG would be the fully loaded carrier transition (4↔5), that effectively parallels 1↔8. Simulations with an arbitrary 50% reduction in k_{45}, k_{54} together with the above changes in δ, gave I–V curves that were consistent with the observed steady-state behavior, including marginal change in Na^+-leak, shift in zero-voltage rates. Moreover, an upward inflexion of the I–V curve with the Na^+-leak subtracted was predicted, in accordance with the I–V data.

Although our model simulations do not allow us to exclude other transitions being modified by PG (e.g., on the cytoplasmic side, the kinetics of which are as yet uncharacterized), the effect of PG treatment of NaPi-IIa can certainly be accounted for by a modification of two translocation steps in the transport cycle. These involve charge and/or substrate translocation between the cis and trans conformations of NaPi-IIa: reduced apparent movement of intrinsic charges (together with a redistribution of the electrical distances associated with first Na^+-binding sites) and deceleration of the fully loaded carrier forward rate constant. We have recently obtained evidence supporting the concept of a single transport pathway through NaPi-IIa (Köhler et al., 2002). These present findings would therefore be consistent with the notion that PG modifies one or more arginine residues associated with the translocation pathway, which lead to reduced voltage dependency and P_i translocation rate.

This work was financially supported by grants awarded to H. Murer from the Swiss National Science Foundation (31-46523), the Fridericus Stiftung (Vaduz, FL-9490) and the Union Bank of Switzerland (Zurich, Bu 704/7-1) and to I. C. Forster from the Hartmann Muller-Stiftung (Zurich).

References

Beck, L., Karaplis, A.C., Amizuka, N., Hewson, A.S., Ozawa, H., Tenenhouse, H.S. 1998. Targeted inactivation of Npt2 in mice leads to severe renal phosphate wasting, hypercalciuria and skeletal annormalities. *Proc. Natl. Acad Sci. USA,* **95:**5372–5377

Bezanilla, F. 2000. The voltage sensor in voltage-dependent ion channels. *Physiol. Rev.* **80:**555–592

Brocke, L., Bendham, A., Grunewald, M, Kanner, B.I. 2002. Proximity of two oppositely oriented reentrant loops in the glutamate transporter GLT-1 identified by paired cyteine mutagenesis. *J. Biol. Chem.* **277:**3895–3992

Chameau, P., Bournard, R., Shimahara, T. 1995. Asymmetric intramembrane charge movement in mouse hippocampal pyramidal cells. *Neurosci. Lett.* **201:**159–162

Etter, E.F. 1990. The effect of phenylglyoxal on contraction and intramembrane charge movement in frog skeletal muscle. *J. Physiol.* **421:**441–462

Forster, I., Wagner, C.A., Busch, A.E., Lang, F., Biber, J., Hernando, N., Murer, H., Werner, A. 1997. Electrophysiological characterization of the flounder type II Na^+/P_i cotrans-

[2] Fitting a single exponential to the presteady-state relaxations is an oversimplification because the total charge movement arises from three voltage-dependent transitions (7↔8, 1↔2, 1↔8), each of which would contribute eigenvalues to the system. Attempts to fit two exponentials to the relaxations, commencing within 1–2 msec of the voltage-step onset were found to be unreliable because of the closeness of the two predicted τs, variability between cells and signal-to-noise ratio available. Similarly, fitting a single Boltzmann function to the Q–V data assumes the system can be reduced to single-transition so that the estimate of z would represent a weighted average of charge movements from all transitions involved. The small apparent valency of NaPi-IIa compared to other Na^+-driven cotransport systems (e.g., SGLT-1) (Loo et al., 1993) and concomitantly flattened Q–V curves has impeded attempts to fit more than one Boltzmann function to the Q–V data (I.C. Forster, unpublished observations).

porter (NaPi-5) expressed in *Xenopus laevis* oocytes. *J. Membrane Biol.* **160:**9–25

Forster, I., Hernando, N., Biber, J., Murer, H. 1998. The voltage dependence of a cloned mammalian renal type II Na^+/P_i cotransporter (Na^+Pi-2). *J. Gen. Physiol.* **112:**1–18

Forster, I., Loo, D.D.F., Eskandari, S. 1999a. Stoichiometry and Na^+ binding cooperativity of rat and flounder renal type II Na^+-P_i cotransporters. *Am. J. Physiol.* **276:**F644–F649

Forster, I., Traebert, M., Jankowski, M., Stange, G., Biber, J., Murer, H. 1999b. Protein kinase C activators induce membrane retrieval of type II Na-phosphate cotransporters expressed in *Xenopus* oocytes. *J. Physiol.* **517:**327–340

Forster, I.C., Biber, J., Murer, H. 2000. Proton sensitive interactions with the type II Na^+/P_i cotransporter. *Biophys. J.* **79:**215–230

Gross, E., Harkins, K., Pushkin, A., Sassani, P., Dukkipati, R., Abuladze, N., Hopfer, U., Kurtz, I. 2001. Phosphorylation of Ser(982) in the sodium bicarbonate cotransporter kNBC1 shifts the HCO_3^-: Na^+ stoichiometry from 3:1 to 2:1 in murine proximal tubule cells. *J. Physiol.* **537:**659–65

Hirsch, J., Loo, D.D.F., Wright, E.M. 1996. Regulation of Na^+/glucose cotransporter expression by protein kinases in *Xenopus* oocytes. *J. Biol. Chem.* **271:**14740–14746

Karlin, A., Akabas, M. 1998. Substituted-Cysteine Accessibility Method. *Meth. Enzym.* **293:**123–145

Köhler, K., Forster, I.C., Stange, G., Biber, J., Murer, H. 2002. Identification of functionally important sites in the 1st intracellular loop of the NaPi-IIa cotransporter. *Amer. J. Physiol. Renal Physiol.* **282:**F687–F696

Lambert, G., Traebert, M., Hernando, N., Biber, J., Murer H. 1999b. Studies on the topology of the renal type II NaPi-cotransporter. *Pflügers Arch.* **437:**972–978

Lambert, G., Forster, I.C., Biber, J., Murer, H. 1999a. Properties of the mutant Ser-460-Cys implicate this site in a functionally important region of the type IIa Na^+/P_i cotransporter protein. *J. Gen. Physiol.* **114:**637–651

Lambert, G., Forster, I.C., Stange, G., Köhler, K., Biber, J., Murer, H. 2001. Cysteine mutagenesis reveals novel structure-function features in the 3rd extracellular loop of NaPi-IIa. *J. Gen. Physiol.* **117:**533–546

Loo, D.D.F., Hazama, A., Supplisson, S., Turk, E., Wright, E.M. 1993. Relaxation kinetics of the Na^+/glucose cotransporter. *Proc. Natl. Acad. Sci. USA.* **90:**5979–5983

Meves, H., Rubly, N., Stämpfli, R. 1988. The action of arginine specific reagents on ionic and gating currents in frog myelinated nerve. *Biochim. Biophys. Acta.* **943:**1–12

Murer, H., Hernando, N., Forster, I., Biber, J. 2000. Proximal tubular phosphate reabsorption: Molecular mechanisms. *Physiol. Rev.* **80:**1373–1409

Parent, L., Supplisson, S., Loo, D.D.F., Wright, E.M. 1992. Electrogenic properties of the cloned Na^+/glucose cotransporter: II A transport model under nonrapid equilibrium conditions. *J. Membr. Biol.* **125:**63–79

Silverman, M. 2000. Glucose reabsorption in the kidney: molecular mechanism of the Na^+/glucose cotransporter. *In*: The Kidney, Physiology and Pathophysiology. D.W. Seldin and G. Giebisch, editors. Raven, New York, pp 2167–2177

Strévey, J., Brunette, M.G., Beliveau, E. 1984. Effect of modification on kidney brush-border-membrane transport activity. *Biochem. J.* **223:**793–802

Strévey, J., Vachon, V., Beaumier, B., Giroux, S., Beliveau, R. 1992. Characterization of essential arginine residues implicated in the renal transport of phosphate and glucose. *Biochim. Biophys. Acta.* **1106:**110–116

Werner, A., Biber, J., Forgo, J., Palacin, M., Murer, H. 1990. Expression of renal transport systems for inorganic phosphate and sulfate in *Xenopus laevis* oocytes. *J. Biol. Chem.* **265:**12331–12336

Wright, E.M., Hirsch, J.R., Loo, D.D.F., Zampighi, G.A. 1997. Regulation of Na^+/glucose cotransporters. *J. Exp. Biol.* **200:**287–293